^{2}H-NMR Spectroscopy of Tunneling Ammonium Ion: General Site Symmetry

Zdzislaw T. Lalowicz

Institut für Physikalische Chemie der Universität, D-4400 Münster*
and Institute of Nuclear Physics, Kraków

Z. Naturforsch. **43a**, 895–907 (1988); received July 19, 1988

^{2}H-NMR powder spectra of tunneling ammonium-d_4 ions are computed. A representation of the tunneling Hamiltonian is worked out in the basis of simple product spin wavefunctions. Secular parts of quadrupole and dipole Hamiltonians are taken into account. Examples of spectra are given for tunneling about one C_2 or C_3 axis, as well as for overall rotations in potentials of higher symmetry. Ranges of tunneling frequencies measurable from the spectra are given for each case. Characteristic shapes of the spectra allow recognition of various ground torsional level structures. Possible further applications and available data are discussed.

PACS number 76.60

I. Introduction

We consider systems of protons ($I = 1/2$) or deuterons ($I = 1$) in solid, diamagnetic nonconducting compounds. In evaluating the spectra we restrict ourselves to dipole-dipole or quadrupole interactions. The dipole-dipole interaction of nuclear dipole moments couples all spins of a system. The interaction of a nuclear quadrupole moment with an electric field gradient (EFG) has single particle character. Comparison of protonated and deuterated systems allows for making use of the differences. Rigid systems of N protons show characteristic features in the NMR spectra for $N = 2$, 3 and 4, whereas for higher N these features are lost [1]. On the other hand, any number of deuterons in a rigid system gives a single doublet spectrum, provided no differences in the EFG exist.

The study of molecular reorientation is based on its specific averaging effect on the spectra. Inclusion of tunneling requires quantum mechanical treatment in terms of space coordinates. The symmetrised wavefunctions of a multispin molecule may be labelled with the irreducible representations of the molecular symmetry group. Except for diatomic molecules, states of different symmetry are coupled by molecular hyperfine interactions. This is of basic importance not only for spin conversion and relaxation processes, but also for the spectra.

The NMR spectrum of a two proton system was calculated by G. E. Pake as early as 1948 [2]. It is commonly called Pake's doublet, in which the separation ν_d defines the dipole-dipole coupling constant C_d: $\nu_d = 3C_d = \frac{3}{2}\frac{\mu_0}{4\pi}\hbar\gamma^2 r^{-3}$. The dipole-dipole interaction is not modulated by reorientation jumps over π. Alternatively, jumps by $\frac{\pi}{2}$ or rotation reduce the doublet splitting by $\frac{1}{2}$. The ^{2}H-NMR spectrum of a rigid pair of deuterons resembles a Pake's doublet with a separation $\delta = \frac{3}{4}C_Q$, scaled up due to a bigger coupling constant $C_Q = e^2 q Q h^{-1}$ by two orders of magnitude. The spectrum is sensitive to jumps by π for an inpressively wide range of exchange rates. The resulting temperature dependence of the correlation time was measured for heavy water molecules in $Li_2SO_4 \cdot D_2O$ [3].

Andrew and Bersohn [4] supplied spectra for a three $I = 1/2$ triangular spin system. They consist of a central line flanked by two side components. The separation of the sidepeaks is reduced by $\frac{1}{2}$ on reorientation about the C_3 symmetry axis. The methyl group CH_3 has often been studied. Slow tunneling frequencies, $\nu_t < 0.1$ MHz, are obtained from the spectra. Fast tunneling rotation was found to give spectra identical to those of fast reorientation [5]. On the other hand, new features were found recently in the NMR spectra of CD_3, which allow identification of the type of motion [6].

The four spins of an ammonium ion form a tetrahedron. The proton NMR lineshapes were treated theoretically for rigid NH_4^+ by Bersohn and Gutowsky [7],

* Alexander von Humboldt Foundation Fellow 1985–87.

Reprint requests to Dr. Z. T. Lalowicz, Institute of Nuclear Physics, ul. Radzikowskiego 152, 31-342 Kraków, Poland.

0932-0784 / 88 / 1000-0895 $ 01.30/0. – Please order a reprint rather than making your own copy.

and the existence of spin isomers was pointed out by Tomita [8]. Three motional cases may be distinguished in a classical analysis of the NMR spectra: rigid ammonium ion, reorientation about its C_3 or C_2 axes and isotropic reorientation [9]. Experimental work of Richards and Schaefer [10] revealed a surprising variety of proton spectra of ammonium compounds at 20 K. These were later explained by tunneling. Formal theoretical treatment and measurements at low temperatures followed [11–13]. The systematics of the spectra according to the ground torsional level (GTL) structure and numerous fits to the low temperature spectra were then supplied [9, 14, 15].

For one-dimensional rotation the torsional energy levels may be calculated from the Mathieu equation with a potential $V_n = \frac{V_0}{2}(1 - \cos n\alpha)$. In the case of ammonium ions a similar calculation may be applied only to one-dimensional rotations about one of its four C_3 or three C_2 symmetry axes. In general, however, ammonium ions may experience potential barriers of various symmetries and thus perform a more complex motion, both in the tunneling rotation and reorientation ranges. A very thorough discussion of a tetrahedron in a cubic crystalline field may be found in the paper by King and Hornig [16]. Smith developed numerical methods to obtain GTL structures for lower symmetry potentials [17]. The complexity and convergence problems in the calculations, as well as idealized forms of potentials lead to poor agreement with experimental data.

There is a need for more data on tunneling frequencies and crystalline potentials. Except for a few cases accessible to the high resolution inelastic neutron scattering (INS) [18], in all remaining cases the GTL structure can be determined for NH_4^+ from the NMR spectra only. NMR remains the only method in the ND_4^+ case, as tunneling splitting is always reduced beyond the resolution of INS methods.

We are going to apply here a group theoretical approach to the GTL structure of ND_4^+. Expressions for GTL energy sublevels are written in terms of parameters representing tunneling frequenices about separate C_3 and C_2 symmetry axes. The tunneling parameters depend on the respective cross sections of a three-dimensional potential. Neither potentials nor tunneling splittings are known, so we use free tunneling parameters. This makes the problem of the NMR spectra of tunneling ND_4^+ ions tractable. The evolution of the spectra on the splittings within the librational ground state multiplet supplies the master forms. Subsequent comparison with experimental spectra should then allow an identification of the GTL structure and in some cases also a determination of the splittings.

An analysis of the NMR spectra of ND_4^+ tunneling in a tetrahedral potential was already presented for single crystals [19] and powder samples [20]. Methods to measure tunnelling frequencies in the $0.1\,\mathrm{MHz} < \nu_t < 20\,\mathrm{MHz}$ range were outlined for $(ND_4)_2SnCl_6$ as an example, but the methods are also applicable to other cubic compounds. These are characterised by the (A, 3T, E) GTL structure, and the tunneling frequency is defined by A to 3T splitting. Most ammonium salts have a crystal symmetry lower than cubic. Lower symmetry barriers lead to other GTL structures at low temperatures and to much more complex reorientation at higher temperatures. Representative examples of both ^{2}H-NMR single crystal and powder spectra are given here for various GTL structures. The sensitivity to ν_t is visualised and the identification of various GTL structures is confirmed.

II. Theoretical Principles

1. Basic Definitions

The calculation of the NMR spectra is based in our treatment on the numerical solution of the eigenvalue problem for a general Hamiltonian. In case of the NMR spectra of deuterated ammonium ions we can limit ourselves to Zeeman, tunneling, quadrupole and dipole-dipole contributions:

$$\mathscr{H} = \mathscr{H}_Z + \mathscr{H}_T + \mathscr{H}_Q + \mathscr{H}_D. \tag{1}$$

Zeeman and tunneling Hamiltonians represent zeroth order energies in spin and space coordinates, respectively. Quadrupole and dipole interactions, bilinear in both coordinates, are acting as perturbations.

We take as starting representation $(2I+1)^4 = 81$ simple product wavefunctions $|I_Z^1 I_Z^2 I_Z^3 I_Z^4\rangle$. Here we will use the notation $I_Z^i = \alpha, 0, \beta$ for $\langle I_z^i\rangle = 1, 0, -1$, respectively, and the superscript i will be recognized from the position. This is the main difference with respect to a previous paper [21], where eigenfunctions of $I = \sum_i |\bar{I}_i|$ and I^2 were used as a basis from the beginning.

We may write the Zeeman Hamiltonian as

$$\mathscr{H}_Z = -\gamma_D \hbar B_0 \sum_{i=1}^{4} I_Z^i. \tag{2}$$

The magnetic quantum number $M = \sum_{i=1}^{4} \langle I_Z^i \rangle$ labels the Zeeman energy levels, and the wavefunctions may be grouped into respective manifolds. A matrix of the Hamiltonian (1) can be structured accordingly, and we get diagonal submatrices of the dimensions $1\times1\,(M=\pm4)$, $4\times4\,(M=\pm3)$, $10\times10\,(M=\pm2)$, $16\times16\,(M=\pm1)$, $19\times19\,(M=0)$ (compare Table 1 in [22]).

The quadrupole interaction Hamiltonian describing the coupling between a non-spherical nuclear charge distribution and the EFG at the nucleus may be written as a product of a Cartesian quadrupole tensor operator Q_{pr} and an EFG tensor $V_{pr} = \dfrac{\partial^2 U}{\partial p\,\partial r}$:

$$\mathscr{H}_Q = \sum_{pr} Q_{pr} V_{pr}, \quad \text{where} \quad p, r = x, y, z \tag{3}$$

with the quadrupole moment $Q_{zz} = e\,Q(\bar{I} \parallel \bar{Z})$ and the maximum principal value $e\,q$ of the EFG V_{pr}. More suitable happens to be an expression of $\mathscr{H}_Q$ as a tensor product of an irreducible spherical tensor of the second rank V_{2m} and the second rank tensor operator Q_{2m},

$$\mathscr{H}_Q = h\,\nu_Q \sum_{\mu=-2}^{2} (-1)^{\mu} Q_{2\mu} V_{2-\mu}, \tag{4}$$

where $\nu_Q = \dfrac{e^2 q Q}{4I(2I-1)h} = \dfrac{1}{4} C_Q$.

Nonsecular $\mu = \pm1, \pm2$ terms mix the states different in M by $\Delta M = \pm1, \pm2$, respectively. Their influence is negligible at high magnetic fields, and only the secular part of (4) is relevant. It may be written as

$$\mathscr{H}_Q^i = h\,\nu_Q\,Q_{20}\,V_{20} = h\frac{C_Q}{8}\,[3I_Z^i I_Z^i - I(I+1)] \cdot(3\cos^2\Theta_i - 1), \tag{5}$$

where the angle Θ_i describes the orientation of the axially symmetric EFG tensor with respect to $\boldsymbol{B}_0$ in the laboratory reference frame.

The Hamiltonian (5) is diagonal in the simple product representation, and the spectrum may be calculated directly. It would represent a sum of spectra for four noninteracting, motionless deuterons.

The secular part of the dipole-dipole interaction

$$\mathscr{H}_D = \sum_{i,j} \frac{\mu_0}{16\pi} \gamma_D^2 \hbar\, r_{i,j}^{-3}\,[I_Z^i I_Z^j - \tfrac{1}{4}(I_+^i I_-^j + I_-^i I_+^j)] \cdot(3\cos^2\Theta_{ij} - 1) \tag{6}$$

fills the diagonal submatrices of the general Hamiltonian with offdiagonal terms. As the contribution of the Hamiltonian (6) to the eigenenergies of the system is relatively small and spoils the clarity of the quadrupole Hamiltonian symmetry, we will henceforth neglect it in the discussion. In the numerical calculations presented further on, the complete Hamiltonian has always been used.

2. *Tunneling Hamiltonian Representation*

The ammonium ion has forms a regular tetrahedron with the nitrogen in the center. There is no evidence of any distortion. We take the center as space-fixed. The T symmetry group has 12 elements, which are rotations about three C_2 and four C_3 symmetry axes, which we take as space fixed. There are A, E and T irreducible representations. These labels help to distinguish various GTL structures. The splittings within the GTLs depend on tunneling parameters and reflect both the strength and symmetry of the crystalline field experienced by the ammonium ion.

A single particle wavefunction $\phi_i(\gamma)$ describes a localisation probability of a particle on an apex (γ) of a tetrahedron pointing into the direction of one of the C_3^i (CRF) axes. A simple product wavefunction $\phi(E) = \phi_1(a)\,\phi_2(b)\,\phi_3(c)\,\phi_4(d)$ describes a ground spatial configuration. Symmetry rotations change the position of the tetrahedron in space, and they are equivalent to permuting $(abcd)$, $C_2^Z \Phi(E) = \phi_1(b)\,\phi_2(a)\,\phi_3(d)\,\phi_4(c) = \Phi(C_2^Z)$. We move about between indistinguishable space states, which are no eigenstates. Similarly we may define simple product spin wavefunctions $\psi_l^M(E) = m_1(a)\;m_2(b)\;m_3(c)\;m_4(d)$, where $M = \sum_i m_i$.

There are 12×81 space-spin simple products. On this basis we may construct convenient linear combinations which have to be invariant under molecular symmetry rotations. A wavefunction

$$\bar{\psi}_l^M = \frac{\sqrt{3}}{6} \sum_{i=1}^{12} \phi(P_i)\,\psi_l^M(P_i) \tag{7}$$

has the required symmetry.

We may define four expectation values of the tunneling Hamiltonian related to rotations about the four C_3^i axes:

$$\Delta(i) = \langle \phi(P_n)\,\psi_l^M(P_j) \,|\, \mathscr{H}_T \,|\, \phi(P_m)\,\psi_k^M(P_k) \rangle, \tag{8}$$

where $P_m = C_3^i P_n$ and $P_k = C_3^i P_j$,

and three rotations about the C_2^x axes:

$$\Pi(\alpha) = \langle \phi(P_n)\psi_l^M(P_j)|\mathscr{H}_T|\phi(P_m)\psi_k^M(P_k)\rangle, \quad (9)$$

where $P_m = C_2^x P_n$ and $P_k = C_2^x P_j$.

The tunneling Hamiltonian describes a degree of overlap between ND_4^+ wavefunctions of neighbouring pocket states. As to the form of $\mathscr{H}_T$ we assume here only that it gives an expectation value between states related by a feasible rotation of the ammonium ion. The tunneling parameters (8) and (9) will be adjusted in the experimentally expectable range.

Representation of $\mathscr{H}_T$ in the basis (7) introduces new blocks within the submatrices labelled by M. There are three kinds of submatrices in the representation of the tunneling Hamiltonian. All are symmetric, and therefore only upper triangle elements are supplied:

$$\begin{array}{c} \\ \left(\begin{array}{cccc} 2\Delta(1) & \Pi(z)+\Delta(3)+\Delta(4) & \Pi(y)+\Delta(2)+\Delta(4) & \Pi(x)+\Delta(2)+\Delta(3) \\ & 2\Delta(2) & \Pi(x)+\Delta(1)+\Delta(4) & \Pi(y)+\Delta(1)+\Delta(3) \\ & & 2\Delta(3) & \Pi(z)+\Delta(1)+\Delta(2) \\ & & & 2\Delta(4) \end{array}\right) \end{array} \begin{array}{ccc} M=3, & M=2, & M=1 \\ |0\alpha\alpha\alpha\rangle, & |\beta\alpha\alpha\rangle, & |\alpha 000\rangle \\ |\alpha 0\alpha\alpha\rangle, & |\alpha\beta\alpha\alpha\rangle, & |0\alpha 00\rangle \\ |\alpha\alpha 0\alpha\rangle, & |\alpha\alpha\beta\alpha\rangle, & |00\alpha 0\rangle \\ |\alpha\alpha\alpha 0\rangle, & |\alpha\alpha\alpha\beta\rangle, & |000\alpha\rangle, \end{array} \quad (10)$$

$$\begin{array}{c} \\ \left(\begin{array}{cccccc} \Pi(z) & \Delta(2)+\Delta(3) & \Delta(2)+\Delta(4) & \Delta(1)+\Delta(3) & \Delta(1)+\Delta(4) & \Pi(x)+\Pi(y) \\ & \Pi(y) & \Delta(1)+\Delta(2) & \Delta(3)+\Delta(4) & \Pi(z)+\Pi(x) & \Delta(1)+\Delta(4) \\ & & \Pi(x) & \Pi(z)+\Pi(y) & \Delta(3)+\Delta(4) & \Delta(1)+\Delta(3) \\ & & & \Pi(x) & \Delta(1)+\Delta(2) & \Delta(2)+\Delta(4) \\ & & & & \Pi(y) & \Delta(2)+\Delta(3) \\ & & & & & \Pi(z) \end{array}\right) \end{array} \begin{array}{cc} M=2, & M=0 \\ |\alpha\alpha 00\rangle, & |\alpha\alpha\beta\beta\rangle \\ |0\alpha 0\alpha\rangle, & |\beta\alpha\beta\alpha\rangle \\ |0\alpha\alpha 0\rangle, & |\beta\alpha\alpha\beta\rangle \\ |\alpha 00\alpha\rangle, & |\alpha\beta\beta\alpha\rangle \\ |\alpha 0\alpha 0\rangle, & |\alpha\beta\alpha\beta\rangle \\ |00\alpha\alpha\rangle, & |\beta\beta\alpha\alpha\rangle, \end{array} \quad (11)$$

$$\begin{array}{c} \\ \left(\begin{array}{ccccccccccc} 0 & \Pi(x) & \Pi(y) & \Pi(z) & \Delta(1) & \Delta(2) & \Delta(3) & \Delta(4) & \Delta(1) & \Delta(2) & \Delta(3) & \Delta(4) \\ & 0 & \Pi(z) & \Pi(y) & \Delta(3) & \Delta(4) & \Delta(1) & \Delta(2) & \Delta(2) & \Delta(1) & \Delta(4) & \Delta(3) \\ & & 0 & \Pi(x) & \Delta(2) & \Delta(1) & \Delta(4) & \Delta(3) & \Delta(4) & \Delta(3) & \Delta(2) & \Delta(1) \\ & & & 0 & \Delta(4) & \Delta(3) & \Delta(2) & \Delta(1) & \Delta(3) & \Delta(4) & \Delta(1) & \Delta(2) \\ & & & & 0 & \Pi(x) & \Pi(y) & \Pi(z) & \Delta(1) & \Delta(4) & \Delta(2) & \Delta(3) \\ & & & & & 0 & \Pi(z) & \Pi(y) & \Delta(3) & \Delta(2) & \Delta(4) & \Delta(1) \\ & & & & & & 0 & \Pi(x) & \Delta(4) & \Delta(1) & \Delta(3) & \Delta(2) \\ & & & & & & & 0 & \Delta(2) & \Delta(3) & \Delta(1) & \Delta(4) \\ & & & & & & & & 0 & \Pi(x) & \Pi(y) & \Pi(z) \\ & & & & & & & & & 0 & \Pi(z) & \Pi(y) \\ & & & & & & & & & & 0 & \Pi(x) \\ & & & & & & & & & & & 0 \end{array}\right) \end{array} \begin{array}{cc} M=1, & M=0 \\ |0\beta\alpha\alpha\rangle, & |\alpha\beta 00\rangle \\ |\alpha\alpha\beta 0\rangle, & |00\beta\alpha\rangle \\ |\alpha\alpha 0\beta\rangle, & |00\alpha\beta\rangle \\ |\beta 0\alpha\alpha\rangle, & |\beta\alpha 00\rangle \\ |0\alpha\beta\alpha\rangle, & |\alpha 0\beta 0\rangle \\ |\alpha\beta\alpha 0\rangle, & |0\beta 0\alpha\rangle \\ |\alpha 0\alpha\beta\rangle, & |0\alpha 0\beta\rangle \\ |\beta\alpha 0\alpha\rangle, & |\beta 0\alpha 0\rangle \\ |0\alpha\alpha\beta\rangle, & |\alpha 00\beta\rangle \\ |\alpha\beta 0\alpha\rangle, & |0\beta\alpha 0\rangle \\ |\beta\alpha\alpha 0\rangle, & |\beta 00\alpha\rangle \\ |\alpha 0\beta\alpha\rangle, & |0\alpha\beta 0\rangle. \end{array} \quad (12)$$

After diagonalizing them we obtain sets of eigenfunctions

$$\Psi_{Gi}^{M} = \sum_j v_{ji} \bar{\psi}_j^M \tag{13}$$

characterised by sets of the symmetry labels G = A, 3T(10), G = A, 3T, 2E(11) and G = A, 9T, 2E(12), respectively. The wavefunctions (13) are properly symmetrised. The applied procedure has led us to smallest possible submatrices of the Hamiltonian (1). We can see which of the simple product wavefunctions are effectively engaged in the symmetry adapted combinations. However, the symmetry adapted wavefunctions (13) are not eigenfunctions of $\bar{I}^2$. Such wavefunctions may be found in [23].

3. *Quadrupole Hamiltonian*

The general features of the quadrupole Hamiltonian may be realized conveniently by considering the symmetry adapted form

$$\begin{aligned}\bar{\mathscr{H}}_Q &= \sum_{i=1}^{4} \bar{\mathscr{H}}_Q^i = \tfrac{1}{4} \sum_{\mathrm{G=A,T_X,T_Y,T_Z}} B_{\mathrm{G}}^0 S_{\mathrm{G}}^0 \\ &= \tfrac{1}{4} \sum_{\mathrm{G}} \left(\sum_{i=1}^{4} a_{\mathrm{G}}^i Q_{20}^i \right) \left(\sum_{i=1}^{4} a_{\mathrm{G}}^i V_{20}^i \right),\end{aligned} \tag{14}$$

where

$$\begin{pmatrix} a_{\mathrm{A}}^i \\ a_{\mathrm{T_X}}^i \\ a_{\mathrm{T_Y}}^i \\ a_{\mathrm{T_Z}}^i \end{pmatrix} = \begin{pmatrix} 1 & 1 & 1 & 1 \\ 1 & -1 & 1 & -1 \\ -1 & 1 & 1 & -1 \\ 1 & 1 & -1 & -1 \end{pmatrix}. \tag{15}$$

We may express V_{20}^i in a suitable common molecular reference frame (MRF) and observe that $\sum_i V_{20}^i = 0$ due to the tetrahedral symmetry. Therefore not only E, but also A terms are not present in (14), and respective levels are not shifted by the quadrupole interaction in the first order.

The second order corrections

$$\delta E_k^{\mathrm{G}} = \sum_{\mathrm{G}'} \sum_l |\langle \Psi_{\mathrm{G}k}^M | \mathscr{H}_Q | \Psi_{\mathrm{G}'l}^M \rangle|^2 / (E_k^{\mathrm{G}} - E_l^{\mathrm{G}'}) \tag{16}$$

exhibit a hyperbolic dependence on the tunneling frequency $-h\nu_t = (E_k^{\mathrm{G}} - E_l^{\mathrm{G}'})$, whereas expectation values in the numerator exist only for (A, T), (T, E) and (T_u, T_w) pairs of (G, G′) symmetry subscripts, provided the T levels are nondegenerate. These cause a fine, tunneling dependent structure of the spectra.

Many of the GTL structures considered here exhibit various degrees of degeneracy, and an adequate perturbation theory approach would be required. Numerical methods give exact solutions in every case.

4. *Symmetry Considerations*

Molecular and crystal field symmetries are essential for the variety of spectra observed for the ammonium ion, both in the temperature ranges of tunneling and reorientation.

In our problem we consider a sample as consisting of crystallites, which are differently oriented with respect to the external magnetic field. Each contains mobile ammonium ions, which are characterised by orientation dependent hyperfine interactions. We have defined the Z direction of the laboratory reference frame (LRF) along the $\bar{B}_0$ direction and, we take the direction of the oscillating RF field as X axis. Let us take a crystal fixed reference frame (CRF) with the z axis coinciding with the Z axis of the LRF. We locate the ammonium ion with its C_2 axes coinciding with the respective CRF axes and label them C_2^{α}, where $\alpha = x, y, z$ and the C_3^i axes pointing into the $[\bar{1}\bar{1}1]$, $[111]$, $[1\bar{1}\bar{1}]$, $[\bar{1}1\bar{1}]$ directions for $i = 1, 2, 3, 4$, respectively. The situation is adequate for the T symmetry of the crystalline field. The difficulty lies in introducing lower symmetries of the potential. The problem is rather complex and confrontable with experimental data in well studied cases only (cf. [24]. We will apply a much simpler approach.

The tunneling frequency depends approximately exponentially on the height of the barrier, however also the slope at the overlap region plays a role. The tunneling parameters Δ and Π reflect the shape of a cross-section through a three-dimensional potential in a plane perpendicular to the axis. We may introduce representative GTL structures by varying the tunneling parameters, among which at most four may be found numerically.

The isotope substitution by deuteration doubles the moment of inertia of the ammonium ion, thus leading to a significant, barrier dependent reduction of the tunneling frequency. It was so far assumed that all splittings within a GTL structure are reduced by the same isotope factor $X = \nu_t^{\mathrm{H}}/\nu_t^{\mathrm{D}}$. That may not be generaly true. The (A-T) and (T-T) tunneling splittings may be reduced by significantly different isotope factors, as already indicated in [25].

One naturally expects structural conclusions to be drawn based on a GTL structure obtained by spectral analysis. It was found, however, that an idea about a barrier is not usually consistent with the point symmetry of the crystal. Ammonium ions, both protonated and deuterated, may exhibit different GTL structures in salts belonging to the same crystallografic class. Possible differences increase with decreasing activation energy. Only in a few cases a clear correspondence was observed [14]. This indicates that we may expect from an analysis of ^{2}H-NMR spectra information about the local symmetry of a barrier only.

III. Results of Computations

1. Single Crystal Spectra

We take as a starting example the most simple case of a cubic crystalline field, resulting for an ammonium ion in the following relations between tunneling parameters: $\Delta = \Delta(1) = \Delta(2) = \Delta(3) = \Delta(4)$, $\Pi(\alpha) \ll \Delta$. The GTL has a (A, 3T, E) structure. The spectra can be clearly separated into symmetry components. NMR transitions within A and E levels contribute to the central component, three pairs of sidebands are purely of T origin at the orientation $\boldsymbol{B}_0 \parallel C_3$ (Figure 1). It is worth while having a closer look at the central line (Figure 2). The spectral components A (two strong central doublets) and E (two outer, overlapping doublets) show a clear, hyperbolic dependence on ν_t, as predicted by (16). This feature was already applied to measure the tunneling frequency in $(ND_4)_2SnCl_6$, both for single crystal [19] and powder [20].

For T components first order shifts define their positions (Figure 1). According to the above symmetry assumptions the 3T levels are degenerate. Splitting some of them will shift the respective components leaving fingerprints on a spectrum's structure, and it may be the main scope to look for in the T spectral components. A single crystal study would allow establishing moderate (< 1 MHz) splittings between T levels. It will be shown elsewhere that $(ND_4)_2SnCl_6$ represents a case of a very slightly distorted cubic crystalline field [25].

We are particularly interested in the spectra for other GTL structures. As before, for NH_4^+ [14] we take various sets of tunneling parameters and obtain some GTL structures, which were found representative. A consistent definition of a tunneling frequency is not possible, but we will keep a mean splitting between A

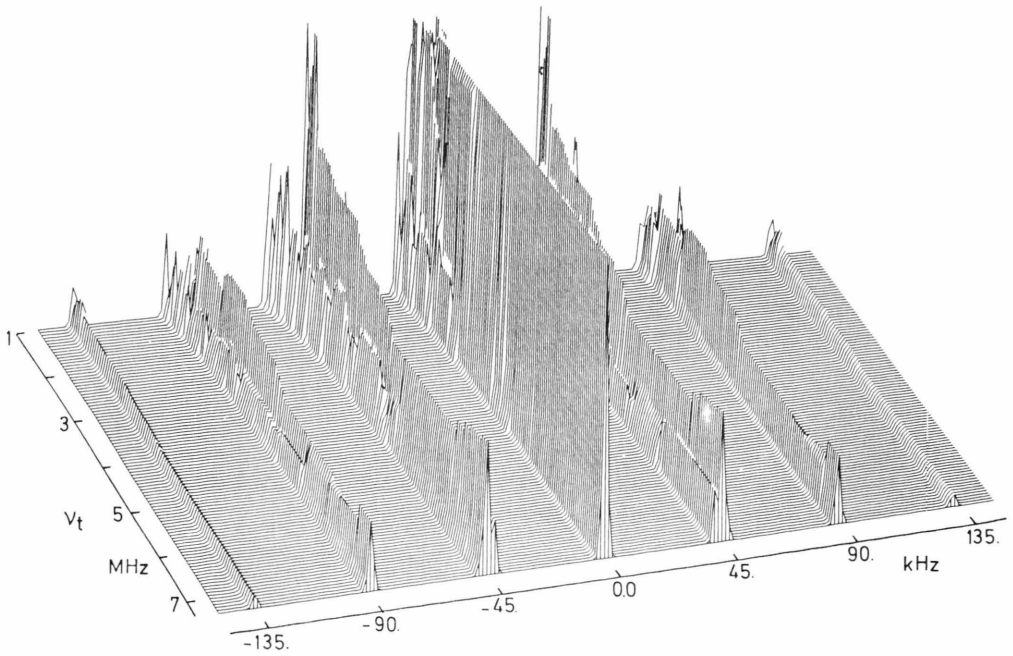

Fig. 1. NMR spectra of ND_4^+ ions oriented with one C_3 axis along the $\boldsymbol{B}_0$ direction. The dependence on the tunneling splitting $h\nu_t$ between A and 3T levels is presented. The spectra are normalized to the maximum amplitude of the central line.

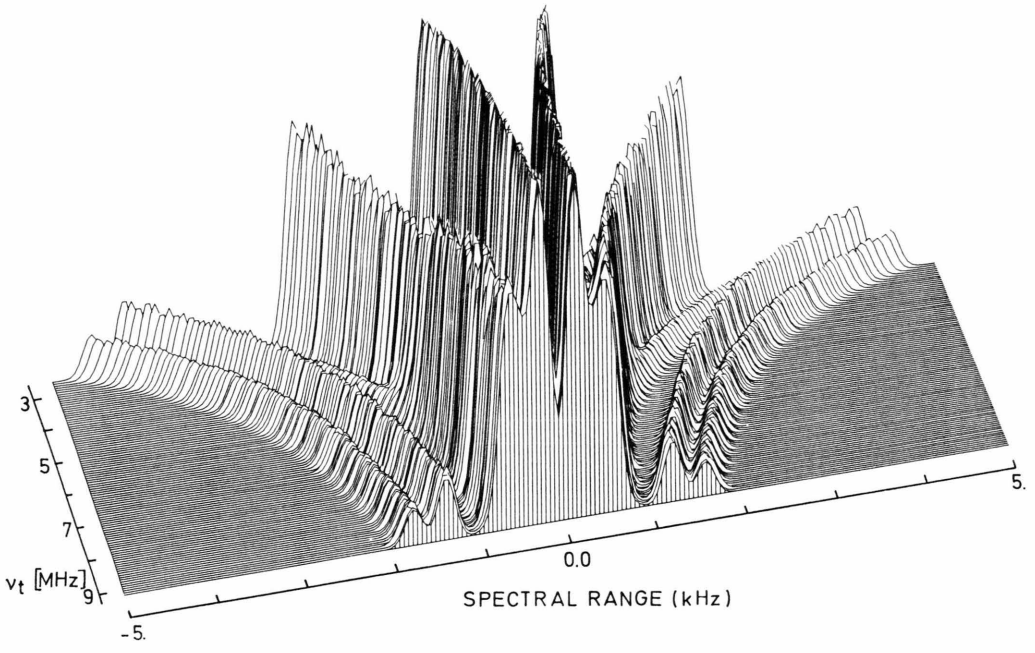

Fig. 2. Dependence of the central component in the spectra of Fig. 1 on the tunneling frequency ν_t.

and T levels at about 5 MHz and between T levels (if split) at about 2 MHz. The positions of the spectral components are not sensitive to any further increase of tunnelling splittings, and the spectra represent only a GTL structure.

Some single crystal spectra are shown in Figure 3. In all cases the orientation $\bar{B}_0 \parallel C_3^2$ was assumed. Lower crystal field symmetry and larger differences between the tunneling parameters produce narrower spectra. It is characteristic that the spectral components are shifted always by a multiple of $C_Q/12 = 15$ kHz. At the chosen orientation the central doublet splitting in the rigid ND_4^+ equals $\frac{1}{2}C_Q$ (Figure 3b).

2. *Powder Spectra*

The ^{2}H-NMR spectrum of the motionless ND_4^+ ion is shown in Figure 4a. The doublet splitting equals $\frac{3}{4}C_Q$. The spectra in Fig. 4 allow to follow the effects due to tunneling about one C_2 axis. The GTL splits into two levels (A + E + T) and 2T separated by $2\Pi(z)$. The splitting in case of Fig. 4b equals 98 kHz. Several spectral components have already moved away from the observation range, and the second moment dropped down to $65.38\, mT^2$ from its rigid lattice value $84.42\, mT^2$ of Figure 4a. The shape, and particularly the doublet with decreasing separation allow estimation of a tunneling splitting up to about 0.3 MHz. At fast enough tunneling a residual spectrum is achieved. Its shape reminds of that of a single $I = 1$ nucleus in a nonaxially symmetric EFG ($\eta = 1$) [26] with reduced quadrupole coupling constant $C'_Q = \frac{1}{2}C_Q$. Tunneling rotation about a C_2 axis averages specifically the quadrupole Hamiltonians of the deuterons to a resultant nonaxial form with a reduced coupling constant. It is worth mentioning at this point that classical reorientation of ND_4^+ ions about a C_2 axis reduces the spectrum to a very narrow central line for $\eta = 0$. Increasing spectral width was observed for $\eta \to 1$ [27].

An evolution of the ^{2}H-NMR spectra on tunneling about one C_3 symmetry axis may be followed on the examples in Figure 5. The two GTL sublevels labelled (A + T) and (E + 2T) are split by $\nu_t = 3\Delta(4)$. At low tunneling frequencies a multicomponent spectrum builds up in the center. The structure of the central line allows accurate determination of ν_t in an intermediate range 0.3 MHz $< \nu_t <$ 0.8 MHz. In the limit of high ν_t, the central doublet separation amounts to one third of the rigid one as a result of the fast exchange of positions of three deuterons. The spectrum of the

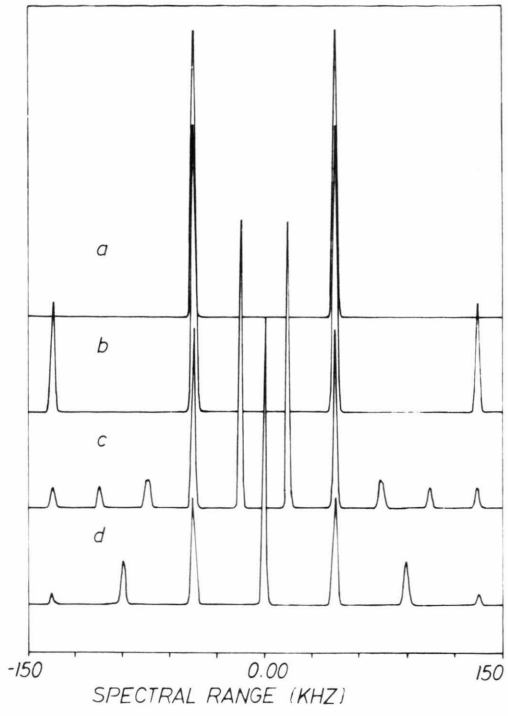

a

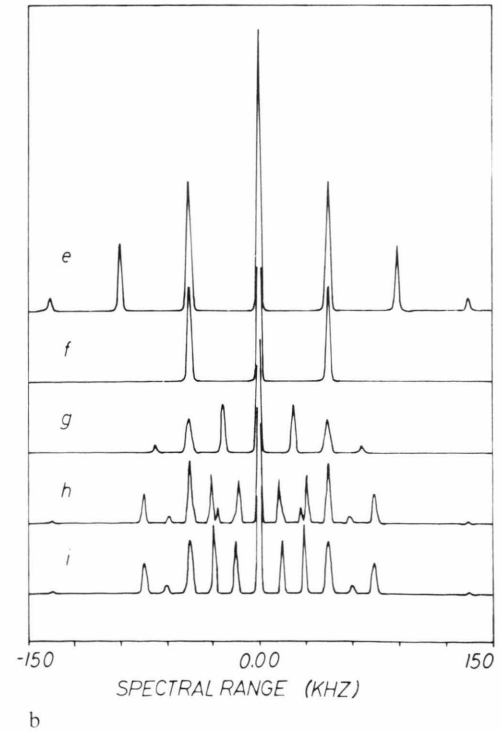

b

fourth, motionless deuteron remains in place. The second moment is reduced to $M_2 = 38.86\, mT^2$. Classical reorientation about a C_3 axis of the ND_4^+ ion leads this time to a slightly different spectrum, and to $M_2 = 36.9\, \mu T^2$ [27]. Significant differences in the ^{2}H-NMR spectra, enabling a clear distinction between tunneling and reorientation of a triangular system of three deuterons may be seen most clearly in CD_3 spectra [6].

In order to proceed systematically with cases of lower symmetry, let us assume that all $\Pi(\alpha) = \Pi$ and $\Delta(i) = 0$. The GTL sublevels (A + E) and 3 T are separated by $\nu_t = 4\Pi$. A strong central doublet is observed for 0.1 MHz $< \nu_t <$ 0.6 MHz (Figure 6). It is the case of D_{2d} potential. The doublet structure is found useful in interpreting complex motions.

In a cubic potential, tunneling about the C_3 axes will dominate and all $\Delta(i) = \Delta$. The GTL structure is now A, 3 T, E (Figure 7). The central line contains now two strong A doublets and practically overlapping two E doublets. Their separations depend inversely on the tunneling frequency $\nu_t = 8\Delta$, allowing its measurement in 0.1 MHz $< \nu_t <$ 6 MHz range [20].

Figure 8 represents examples of spectra obtained when going from the case of Fig. 5 d towards the case of Figure 7 d. Thus, introducing except fast tunneling about the $C_3(4)$ axis also $\Delta' = \Delta(1) = \Delta(2) = \Delta(3)$, we observe four levels in the GTL: A, T, 2 T and E. The splittings are

$$\begin{aligned} E(\mathrm{A}-\mathrm{T}) &= 8\Delta' = \Pi, \\ E(\mathrm{A}-2\mathrm{T}) &= 3\Delta(4) + 5\Delta' + \Pi, \\ E(\mathrm{A}-\mathrm{E}) &= 3\Delta(4) + 9\Delta'. \end{aligned} \tag{17}$$

The spectra allow an estimation of the degree of motional anisotropy. However, even for small splittings

Fig. 3. Examples of single crystal ^{2}H-NMR spectra (ND_4^+ oriented with C_3^2 axis along $\boldsymbol{B}_0$). The following cases are considered (omitted tunneling parameters are zero):

a) $\Pi(z) \gg C_Q$, $M_2 = 47.6\, mT^2$, ($1\, mT^2 = 10^{-6} T^2$)
b) rigid ion, $M_2 = 141.7\, mT^2$,
c) $\Delta(3) \gg C_Q$, $M_2 = 57.6\, mT^2$,
d) $\Pi(x) = \Pi(y) = \Pi(z) \gg C_Q$, $M_2 = 60\, mT^2$,
e) $\Delta(1) = \Delta(2) = \Delta(3) = \Delta(4) \gg C_Q$, $M_2 = 61\, mT^2$,
f) $\Pi(z) > \Pi > \Delta(i) \gg C_Q$, $M_2 = 21.4\, mT^2$,
g) $\Delta(1) = \Delta(2) \neq \Delta(3) = \Delta(4) \gg C_Q$, $M_2 = 14.4\, mT^2$,
h) $C_Q \ll \Delta(1) < \Delta(2) = \Delta(3) = \Delta(4)$, $M_2 = 29.3\, mT^2$,
i) $\Delta(1) > \Delta(2) = \Delta(3) = \Delta(4) \gg C_Q$, $M_2 = 30.1\, mT^2$.

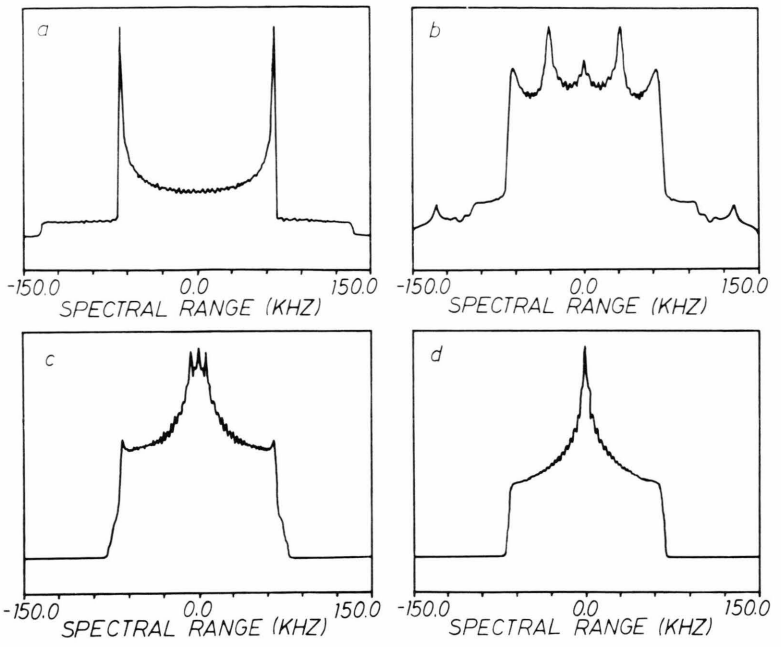

Fig. 4. NMR spectra of ND_4^+ ions in a powder.
a) rigid ion, $M_2 = 84.42\, m T^2$,
Evolution on tunneling about one C_2 axis. Tunneling splitting equals $2\Pi(z)$.
b) $\nu_t = 98$ kHz, $M_2 = 65.4\, m T^2$,
c) $\nu_t = 261.4$ kHz, $M_2 = 33.8\, m T^2$,
d) $\nu_t = 3.2$ MHz, $M_2 = 28.6\, m T^2$.

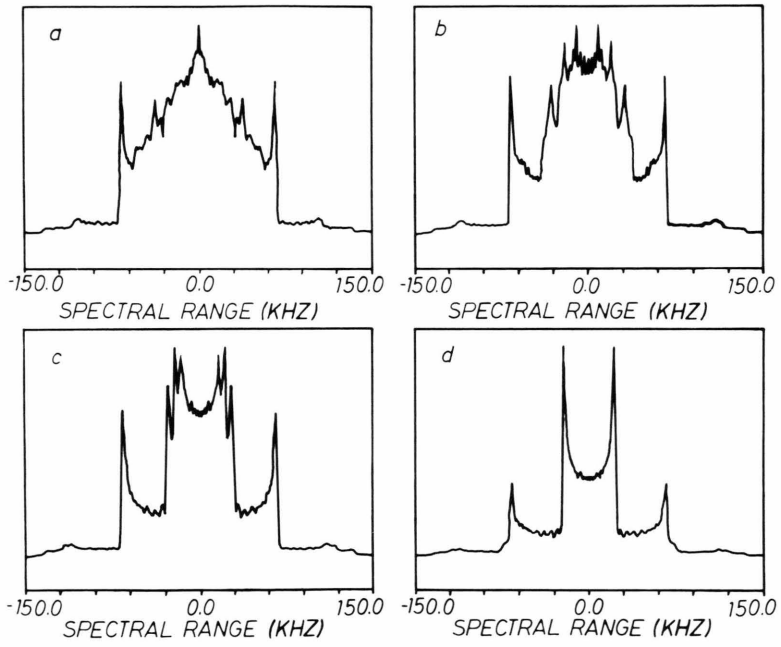

Fig. 5. Evolution of NMR powder spectra of ND_4^+ ions on tunneling frequency about one C_3 axis. Tunneling splitting equals $3\Delta(4)$.
a) $\nu_t = 196$ kHz, $M_2 = 42.9\, m T^2$,
b) $\nu_t = 343$ kHz, $M_2 = 39.6\, m T^2$,
c) $\nu_t = 687$ kHz, $M_2 = 38.8\, m T^2$,
d) $\nu_t = 9.8$ MHz, $M_2 = 38.8\, m T^2$.

within the GTL a role of Π may be not recognisable, as it does not change the distance between T levels.

We may follow an evolution of the spectra between the case of tunneling one C_2 axis (Fig. 4d) towards all C_2 axes equal by tunneling (Fig. 6d) on examples in Fig. 9. The GTL scheme is (A + E), T, 2T with splittings

$$E(\mathrm{A} - \mathrm{T}) = 4\Pi,$$

$$E(\mathrm{A} - 2\mathrm{T}) = 2\Pi(z) + 2\Pi,$$

$$\text{where} \quad \Pi = \Pi(x) = \Pi(y). \tag{18}$$

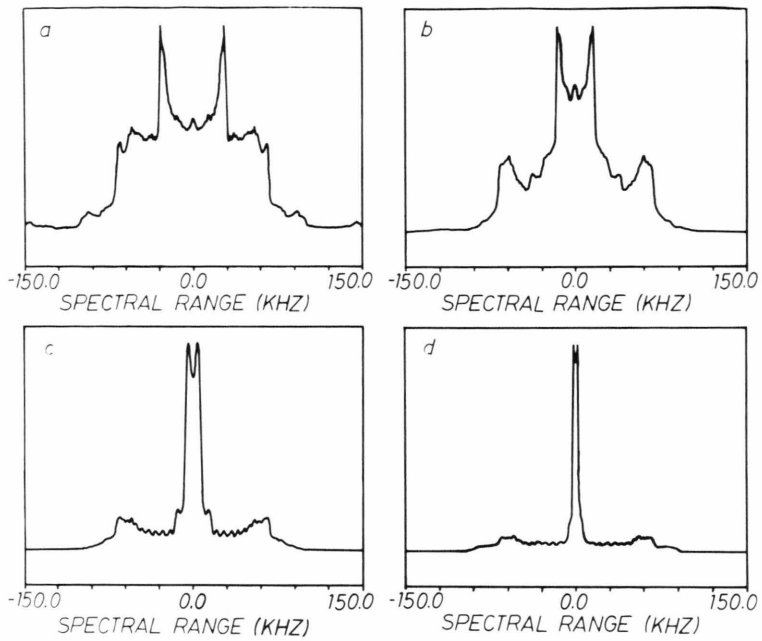

Fig. 6. Evolution of the spectra on equal tunneling frequency about all C_2 axes: $\Pi = \Pi(x) = \Pi(y) = \Pi(z)$. Tunneling splitting equals 4Π.

a) $\nu_t = 130.7\,\text{kHz}$, $M_2 = 53.3\,m\,T^2$,
b) $\nu_t = 261.4\,\text{kHz}$, $M_2 = 35.8\,m\,T^2$,
c) $\nu_t = 784.2\,\text{kHz}$, $M_2 = 32.7\,m\,T^2$,
d) $\nu_t = 1.96\,\text{MHz}$, $M_2 = 32.5\,m\,T^2$.

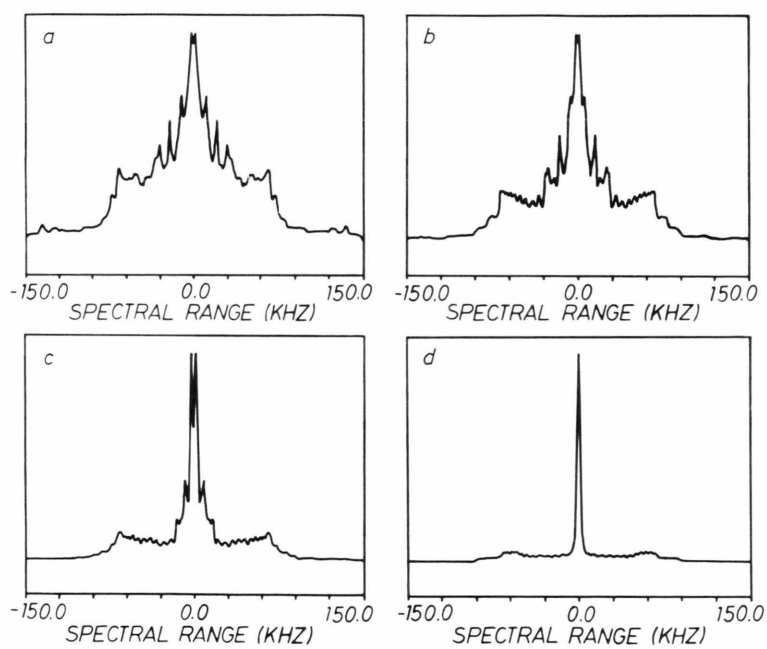

Fig. 7. Evolution of the spectra on equal tunneling frequency about all C_3 axes: $\Delta = \Delta(1) = \Delta(2) = \Delta(3) = \Delta(4)$. Tunneling splitting equals 8Δ.

a) $\nu_t = 183\,\text{kHz}$, $M_2 = 57.3\,m\,T^2$,
b) $\nu_t = 261.4\,\text{kHz}$, $M_2 = 43.6\,m\,T^2$,
c) $\nu_t = 522.8\,\text{kHz}$, $M_2 = 35.8\,m\,T^2$,
d) $\nu_t = 2.61\,\text{MHz}$, $M_2 = 32.9\,m\,T^2$.

The spectrum in Fig. 10a represents again a cubic case with $\Delta = \Delta(1) = \Delta(2) = \Delta(3) = \Delta(4) = 326\,\text{kHz}$. Differentiation among Δ parameters produces effects in the T spectral components. In order to follow the details of their shape more accurately, we have enlarged by a factor of two the amplitude of the spectra in Figs. 10 and 11 and show them with the central line cut off a half the amplitude. The spectra evolve on decreasing $\Delta(4)$ as shown in Figure 10. The GTL has the (A, 2T, T, E) structure. The splitting between 2T and T levels equals $3[\Delta - \Delta(4)]$. The second moment decreases significantly from $M_2 = 32.7\,mT^2$ (Fig. 10a)

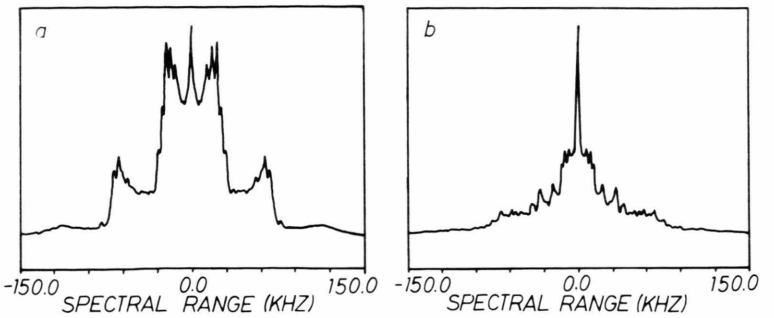

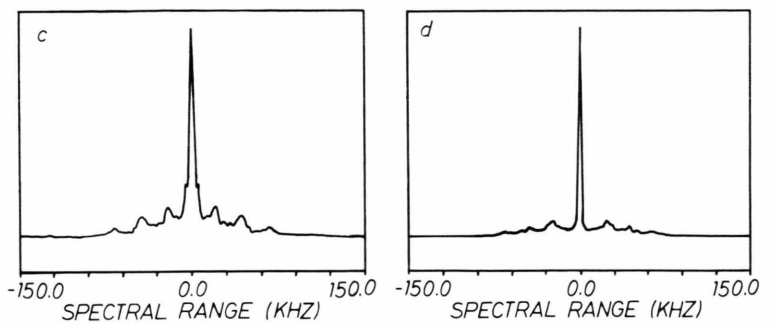

Fig. 8. Evolution of the spectra from the one C_3 axis tunneling case with $\Delta(4) = 0.98$ MHz (Fig. 6d) on increasing tunneling about other C_3 axes $\Delta' = \Delta(1) = \Delta(2) = \Delta(3)$:

a) $\Delta' = 2$ kHz, $M_2 = 38.7\, m\,T^2$,
b) $\Delta' = 6.5$ kHz, $M_2 = 38.7\, m\,T^2$,
c) $\Delta' = 32.6$ kHz, $M_2 = 24.1\, m\,T^2$,
d) $\Delta' = 653.5$ kHz, $M_2 = 18.9\, m\,T^2$.

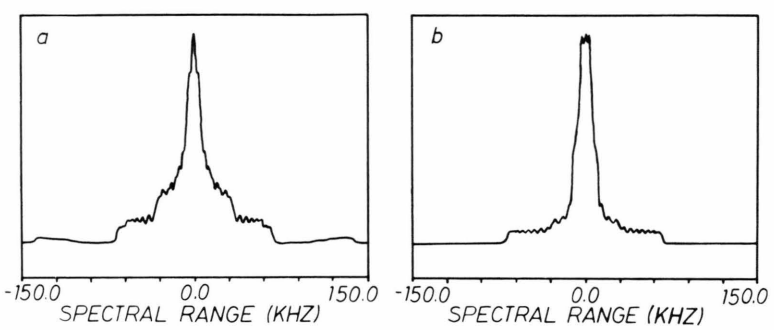

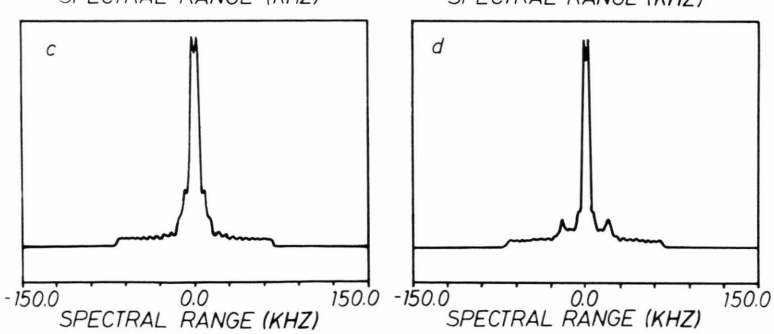

Fig. 9. Evolution of the spectra from the case of one C_2 axis tunneling with $\Pi(z) = 490$ kHz (Fig. 5d) on increasing tunneling about other C_2 axes $\Pi = \Pi(x) = \Pi(y)$:

a) $\Pi = 26.1$ kHz, $M_2 = 28.1\, m\,T^2$,
b) $\Pi = 98$ kHz, $M_2 = 12.2\, m\,T^2$,
c) $\Pi = 261$ kHz, $M_2 = 11.6\, m\,T^2$,
d) $\Pi = 392$ kHz, $M_2 = 13\, m\,T^2$.

to $M_2 = 17.95\, mT^2$ (Fig. 10d), but it seems to be more important to observe the beats on the sidebands. These are also separated by $C_Q/12$. When taking $\Delta(1) = \Delta(2) \neq \Delta(3) = \Delta(4)$, the degeneracy of the T levels is completely removed and they are split symmetrically by $2[\Delta(1) - \Delta(3)]$. As the splitting increases, the narrowest ND_4^+ spectrum is obtained for which $M_2 = 7\, mT^2$ (Figure 11d).

IV. Some Experimental Aspects

The theoretical spectra supplied here represent a variety of experimentally expectable cases. The results

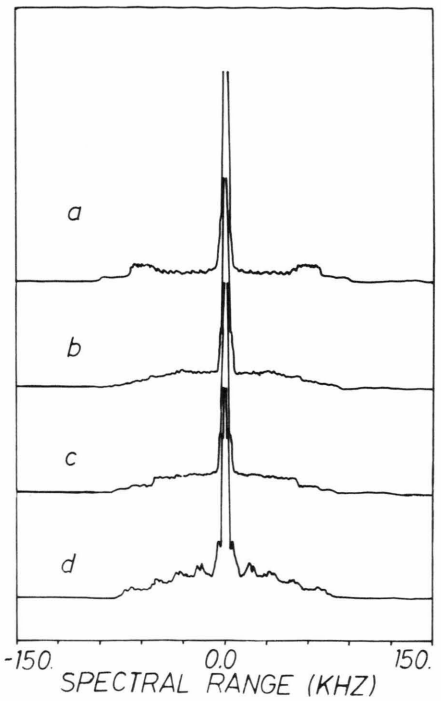

Fig. 10. Some examples of the spectra for (2 T, T) structure, $\Delta' \geq \Delta(4)$:

a) $\Delta' = \Delta(4) = 326.7$ kHz, $M_2 = 32.7\, m\,T^2$,
b) $\Delta' = 326.7$ kHz, $\Delta(4) = 294$ kHz, $M_2 = 29.4\, m\,T^2$,
c) $\Delta' = 326.7$ kHz, $\Delta(4) = 261.4$ kHz, $M_2 = 18.9\, m\,T^2$,
d) $\Delta' = 326.7$ kHz, $\Delta(4) = 65.3$ kHz, $M_2 = 17.9\, m\,T^2$.

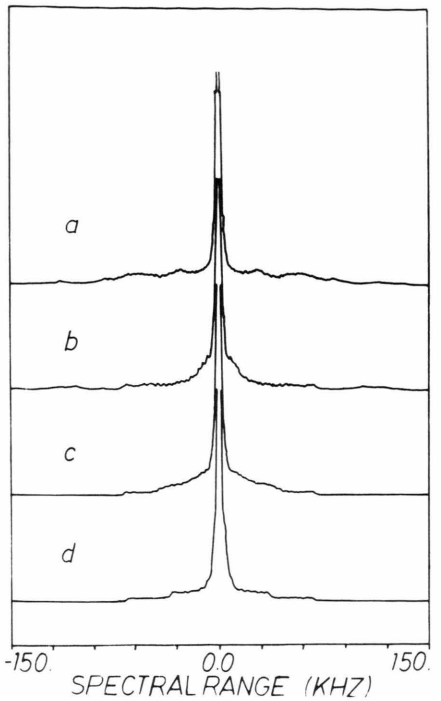

Fig. 11. Examples of the spectra for (T, T, T) structure, $\Delta_1 = \Delta(1) = \Delta(2)$, $\Delta_2 = \Delta(3) = \Delta(4)$:

a) $|\Delta_1 - \Delta_2| = 26.1$ kHz, $M_2 = 31.4\, m\,T^2$,
b) $|\Delta_1 - \Delta_2| = 52.3$ kHz, $M_2 = 24.7\, m\,T^2$,
c) $|\Delta_1 - \Delta_2| = 78.3$ kHz, $M_2 = 11.1\, m\,T^2$,
d) $|\Delta_1 - \Delta_2| = 261.4$ kHz, $M_2 = 7\, m\,T^2$.

are applicable to high magnetic field measurements ($\nu_0 > 20$ MHz) as only the secular quadrupole Hamiltonian has been taken into account.

Although ^{2}H-NMR studies of ammonium ion mobility have already drawn some attention, data on high field NMR spectra are scarce. The aim of most studies was to compare NH_4^+ and ND_4^+ activation energies obtained from T_1 measurements, cf. [28–30], or to get more insight into the mobility in various phases [31–33]. These and similar studies may serve as guidance for a proper selection of samples from the point of view of barrier height, which is only slightly greater for deuterated ammonium ions.

^{2}H-NMR spectra have also been measured at low fields [21, 22, 32, 34, 35]. Two types of spectra were observed: more commonly a broad doublet characteristic for rigid ammonium ions in a powder and narrow asymmetric lines. The latter feature proves the existence of tunneling rotation. We can say now that only the central spectral component was considered. Observed asymmetry was caused by $m = \pm 1, \pm 2$ terms in the quadrupole Hamiltonian. These terms introduce also a dependence of the spectra on the Larmor frequency and imply contingency of tunneling frequency measurements by search for level-crossing conditions $\nu_t = \nu_0$ or $2\nu_0$. In this way, tunneling splittings were first measured for ND_4ClO_4, and the estimated isotope reduction factor of ν_t was X = 300 [34]. The spectra depend on both ν_0 and ν_t and bring about sensitivity problems in experiments and questions about unequivocality of fits.

The data presented in [20] indicate advantages of the high field case as measurements are easier and interpretation of the spectra is much simpler, both making the evaluation of ν_t more straightforward. So far a complete study of ^{2}H-NMR spectra at high and low fields for both single crystal and powder was presented for $(ND_4)_2SnCl_6$. A tunneling frequency $\nu_t = 7.1$ MHz was measured and the reduction factor was found to be about 100 [19].

Other suitable examples may be selected among ammonium salts with barriers below about 4 kJ/mol.

As crystal structures at low temperatures are known only in a few cases, proton NMR spectra may be used as a guidance, [14, 15 and references therein]. Tunneling splittings and GTL structures gained from analysis of spectra may give insight into their dependence on the height and shape of the barrier. Work along these lines is in progress.

The spectra disclose two processes on increasing temperature. The first one is related to decreasing tunneling frequency. The second is due to motional narrowing. As far as ν_t is sufficiently large, only the T spectral components show up effects of reorientation [36]. Under permitting conditions, i.e. when $\nu_t = 0$ and the reorientation rate is negligible, a rigid case may be observed at the border temperature between the tunneling and thermally activated reorientation ranges. The picture depends on the barrier heights. With decreasing barrier the motional narrowing starts at lower and lower temperatures. In some cases it may start at helium temperatures. In such cases the spectra would exhibit in their temperature dependence combined effects of both tunneling frequency and correlation.

A variety of spectra may be observed for high barrier ammonium salts at sufficiently high temperatures before reaching the narrow line characteristic for isotropic reorientation. So far these were analysed only in terms of ammonium ion deformation [26, 31]. Motional narrowing effects in the spectra of ND_4^+ due to anisotropic reorientation, which offer a new explanation, will be presented elsewhere [37].

^{2}H-NMR spectroscopy offers several ways of getting insight into fine features of both tunneling rotation and classical reorientation.

Acknowledgement

Computations were performed on account of the Institute of Physical Chemistry at the University of Münster. The Author would like to express his appreciation of hospitality and cooperation of Professor W. Müller-Warmuth and members of the NMR group.

[1] D. B. Zax, A. Bielecki, K. W. Zilm, A. Pines, and D. P. Weitekamp, J. Chem. Phys. **83,** 4877 (1985).
[2] G. E. Pake, J. Chem. Phys. **16,** 327 (1948).
[3] B. Berglund and J. Tegenfeldt, J. Mag. Res. **27,** 315 (1977).
[4] E. R. Andrew and R. Bersohn, J. Chem. Phys. **18,** 159 (1950).
[5] F. Apaydin and S. Clough, J. Phys. C: Solid St. Phys. **1,** 932 (1968).
[6] Z. T. Lalowicz, U. Werner, and W. Müller-Warmuth, Z. Naturforsch **43a,** 219 (1988).
[7] R. Bersohn and H. S. Gutowsky, J. Chem. Phys. **22,** 651 (1954).
[8] K. Tomita, Phys. Rev. **89,** 429 (1953).
[9] Z. T. Lalowicz, C. A. McDowell, and P. Raghunathan, J. Chem. Phys. **68,** 852 (1978).
[10] R. E. Richards and R. Schaefer, Trans. Faraday Soc. **57,** 201 (1961).
[11] A. Watton and H. E. Petch, Phys. Rev. **B7,** 12 (1973).
[12] R. Ikeda and C. A. McDowell, Mol. Phys. **25,** 1217 (1973).
[13] M. Punkkinen, J. Tuohi, and E. E. Ylinen, J. Mag. Res. **22,** 527 (1976).
[14] Z. T. Lalowicz, C. A. McDowell, and P. Raghunathan, J. Chem. Phys. **70,** 4819 (1979), Erratum ibid. **72,** 3443 (1980).
[15] Z. T. Lalowicz, Acta Phys. Polon. **A56,** 243 (1979).
[16] H. F. King and D. F. Hornig, J. Chem. Phys. **44,** 4520 (1966).
[17] D. Smith, J. Chem. Phys. **68,** 619 (1978).
[18] W. Press, Single Particle Rotations in Molecular Crystals, Springer Tracts in Modern Physics, **92** (1981).
[19] L. P. Ingman, E. Koivula, Z. T. Lalowicz, M. Punkkinen, and E. E. Ylinen, Z. Phys. B: Condensed Matter **66,** 363 (1987).
[20] L. P. Ingman, E. Koivula, Z. T. Lalowicz, M. Punkkinen, and E. E. Ylinen, J. Chem. Phys. **88,** 58 (1988).
[21] J. S. Blicharski, Z. T. Lalowicz, and W. T. Sobol, J. Phys. C: Solid St. Phys. **11,** 4187 (1978).
[22] Z. T. Lalowicz and W. T. Sobol, J. Phys. C: Solid St. Phys. **16,** 2352 (1983).
[23] D. van der Putten and N. J. Trappeniers, Physica **129A,** 302 (1985).
[24] W. Müller and A. Hüller, J. Phys. C: Solid State Phys. **15,** 7295 (1982).
[25] L. P. Ingman, E. Koivula, Z. T. Lalowicz, M. Punkkinen, and E. E. Ylinen, Z. Phys. B: Condensed Matter, Part II (submitted).
[26] T. Chiba, J. Chem. Phys. **36,** 1122 (1962).
[27] J. S. Blicharski, Z. T. Lalowicz, and W. T. Sobol, Acta. Phys. Polon. **A54,** 581 (1978).
[28] D. J. Genin and D. E. O'Reilly, J. Chem. Phys. **1969,** 2842.
[29] L. Niemelä and T. Lohikainen, Phys. kondens. Materie **6,** 376 (1967).
[30] L. Niemelä and P. H. Oksman, Chem. Phys. Lett. **41,** 174 (1976).
[31] V. Hovi, U. Järvinen, and P. Pyykkö, Ann. Acad. Sci. Fenn. **AVI,** 221 (1966).
[32] L. Niemelä and J. Tuohi, Ann. Acad. Sci. Fenn. **AVI,** 137 (1970).
[33] S. Damle, L. C. Gupta, and R. Vijayaraghavan, Chem. Phys. Letters **37,** 614 (1976).
[34] Z. T. Lalowicz, J. Phys. C: Solid St. Phys. **16,** 2363 (1983).
[35] R. R. Knispel, H. E. Petch, and M. M. Pintar, Solid State Commun. **11,** 679 (1972).
[36] L. P. Ingman, E. Koivula, Z. T. Lalowicz, M. Punkkinen, and E. E. Yinen, Quantum Aspects of Molecular Motions in Solids, A. Heidemann, A. Magerl, M. Prager, D. Richter, and T. Springer, Eds. Springer Proceedings in Physics **17,** 122 (1987).
[37] Z. T. Lalowicz and S. F. Sagnowski (to be published).

Verantwortlich für den Inhalt: A. KLEMM
Satz und Druck: Konrad Triltsch, Würzburg